Journal of Medicinal Chemistry

Article

DESIGN AND CHARACTERIZATION OF NOVEL COVALENT BROMODOMAIN AND EXTRA-TERMINAL DOMAIN (BET) INHIBITORS TARGETING A METHIONINE

Olesya Kharenko, Reena G Patel, S. David Brown, Cyrus Calosing, Andre White, Damodharan Lakshminarasimhan, Robert K Suto, Bryan C Duffy, Douglas B. Kitchen, Kevin G McLure, Henrik C. Hansen, Edward H van der Horst, and Peter R. Young

J. Med. Chem., **Just Accepted Manuscript** • DOI: 10.1021/acs.jmedchem.8b00666 • Publication Date (Web): 30 Aug 2018

ACS Publications

is published by the American Chemical Society. 1155 Sixteenth Street N.W., Washington, DC 20036

DESIGN AND CHARACTERIZATION OF NOVEL COVALENT BROMODOMAIN AND EXTRA-TERMINAL DOMAIN (BET) INHIBITORS TARGETING A METHIONINE

Olesya A. Kharenko[a], Reena G. Patel[a], S. David Brown[a], Cyrus Calosing[a], Andre White[b], Damodharan Lakshminarasimhan[b], Robert K. Suto[b], Bryan C. Duffy[c], Douglas B. Kitchen[c], Kevin G. McLure[a], Henrik C. Hansen[a], Edward H van der Horst[a], Peter R. Young[a]*

a Zenith Epigenetics, Suite 300, 4820 Richard Road SW, Calgary, Alberta, T3E 6L1, Canada

b Xtal BioStructures, Inc., 12 Michigan Dr., Natick, MA 01760, USA

c AMRI, 26 Corporate Circle, PO Box 15098, Albany, NY 12212-5098, USA

KEYWORDS: BRD4, Bromodomains, BET Inhibitors, Covalent Inhibitor, Methionine

ABSTRACT

BET proteins are key epigenetic regulators which regulate transcription through binding to acetylated lysine (AcLys) residues of histones and transcription factors through bromodomains (BDs). The disruption of this interaction with small molecule bromodomain inhibitors is a promising approach to treat various diseases including cancer, autoimmune and cardiovascular diseases. Covalent inhibitors can potentially offer a more durable target inhibition leading to improved in vivo pharmacology. Here we describe the design of covalent inhibitors of BRD4(BD1) that target a methionine in the binding pocket by attaching an epoxide warhead to a suitably oriented non-covalent inhibitor. Using thermal denaturation, MALDI-TOF mass spectrometry and an X-ray crystal structure, we demonstrate that these inhibitors selectively form a covalent bond with Met149 in BRD4(BD1) but not other bromodomains, and provide durable transcriptional and anti-proliferative activity in cell based assays. Covalent targeting of methionine offers a novel approach to drug discovery for BET proteins and other targets.

INTRODUCTION

BET proteins are epigenetic readers, which regulate gene transcription by interacting with acetylated lysine (AcLys) residues of histones and transcription factors through bromodomains, evolutionarily conserved protein domains that have recently emerged as key epigenetic regulators of gene transcription[1]. BET proteins consist of a family of four proteins, BRD2, BRD3, BRD4 and BRDT that each contains two tandem bromodomains (BD1) and (BD2). Inhibition of BET protein binding to acetylated histones can effect the transcription of genes involved in various diseases including different types of cancer, cardiovascular and auto-immune diseases.[2] Most BET inhibitors (BETi) are small molecules designed to reversibly interact with the bromodomains of the BET proteins and disrupt their interaction with the acetylated lysine residues, and several candidate BETi have advanced into clinical development for multiple indications,[3] including cancer indications such as acute myeloid leukemia, multiple myeloma, non-Hodgkin's lymphoma, and various solid tumors.[4]

Recently, proteolytic targeting chimera (PROTAC)-induced degradation of BRD4 has been described as a novel and promising therapeutic strategy for BET inhibition.[5] The principle of this approach is a complete degradation of BRD4 through the PROTAC containing the BET protein recognition unit and an ubiquitin ligase recognition module. Several reports show that complete degradation of BRD4 through PROTAC results in superior potency, prolonged downregulation of MYC, as well as lasting anti-proliferative effects and induction of cell death in multiple cancer cell lines.[6-10] However these molecules are large which may preclude oral delivery.

Covalent inhibitors have been widely used as successful drug therapies in various indications,[12, 13] also offering similar advantages including increased duration of action, prolonged target

modulation, and potential pharmacological effect at lower concentrations (e.g. ibrutinib).[14] Like PROTAC technology, the durability of the pharmacological effect depends on the synthesis of new protein but also includes a possible dominant negative effect due to the durability of the drug-target protein. Target specificity is obtained by combining a selective non-covalent inhibitor with a weakly reactive warhead that can target a proximal, typically nucleophilic amino acid such as lysine, serine, threonine or cysteine, with the latter particularly attractive due to its relatively low abundance leading to greater specificity. Examples include ibrutinib, afatinib and rociletinib.[15] Zhong et al. have described the development of irreversible BET inhibitors.[11] A metal-based BET inhibitor was designed to bind irreversibly to histidine amino acid residues of BRD4. Even though the approach of the irreversible covalent BET inhibition was novel, the X-ray co-crystal structure of the obtained adduct remains elusive and the exact interacting amino acid residue has yet to be determined. Daguer at al. have described promiscuous covalent probes capable of binding to cysteine amino acid residues across the family of bromodomains suggesting the possibility of the covalent targeting of several bromodomains through this approach.[16]

To date, methionine has not been considered an amino acid to target with a covalent inhibitor. Here we describe the rational design and characterization of a novel series of covalent BET inhibitors targeting amino acid residue Met149 in the binding site of BRD4, which demonstrate promising durable inhibitory effects on proliferation in vitro and sustained effects on target modulation. We show beneficial effects of our covalent approach for BET inhibition, which can potentially lead to novel and more effective cancer therapy as well as providing an alternative strategy for covalent inhibitor design.

RESULTS AND DISCUSSION

In order to assess the possibility of rationally designing a covalent BET inhibitor, we evaluated various co-crystal structures of inhibitors with BRD4(BD1) including the co-crystal structure of **1** (**ZEN-2759)** bound to BRD4(BD1), which was obtained at 1.88 Å resolution (Figure 1). The crystal structure shows that the dimethyl-isoxazole group of **1** is involved in key interactions within the binding site, by forming a H-bond (3.1 Å) with the amide nitrogen of Asn140 and a water-mediated H-bond to the hydroxyl group of Tyr97. While there was not a cysteine located near the binding site, the benzyl's 4-position of **1** was positioned in good proximity to the Met149 residue (3.9 Å). While methionine has never been targeted before for covalent drug design, Alferiev et al. have previously described epoxides with high reactivity towards methionine and other aliphatic sulfides in physiological conditions, which resulted in the formation of sulfonium complexes,[17] suggesting that it might be possible to attach an epoxide to a reversible inhibitor to obtain a covalent drug. We then docked proposed substitutions of **1** into the binding site of BRD4(BD1). In those cases where the epoxide appeared close enough for Met149 to react, the expected bond was formed and the complex minimized by a small sphere of free atoms. Those compounds that were predicted to exert minimal strain in the binding site in both noncovalent and reacted states were then considered for synthesis (Figure 2). A similar process was conducted using in silico methods with **2** and **3**.

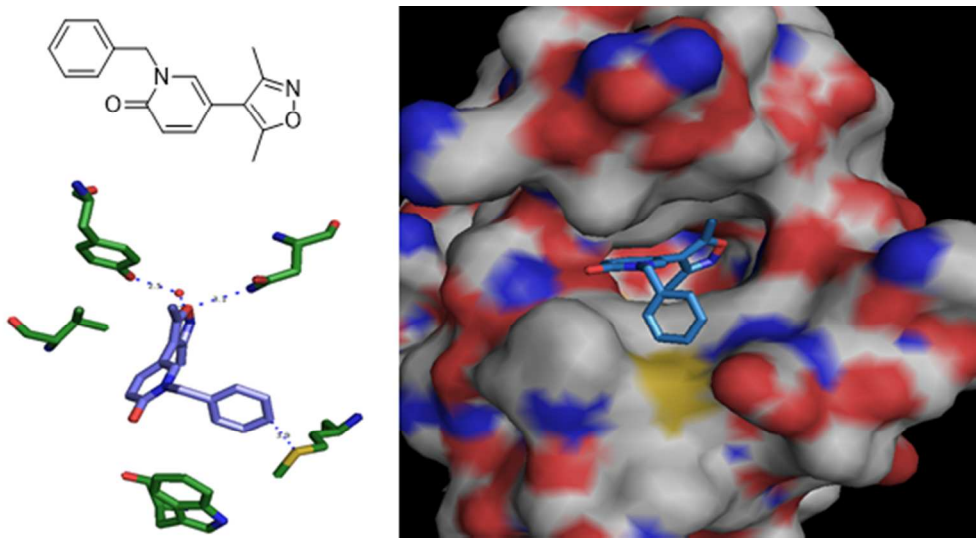

Figure 1. The chemical structure of **1** (**ZEN-2759)** (top left). Co-crystal structure of BRD4(BD1) and **1**, pdb code 6CZV.pdb, showing specific protein-ligand interactions (bottom left) and a surface representation (right).

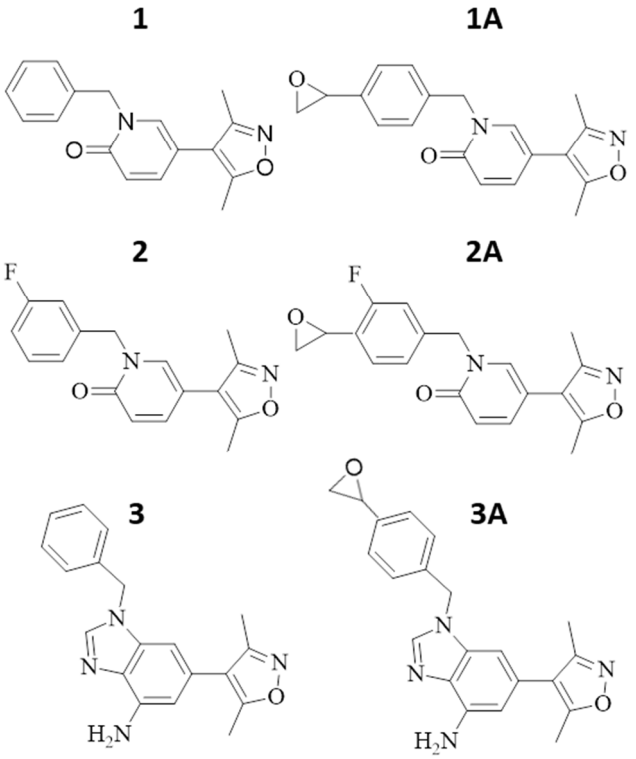

Figure 2. Chemical structures of epoxide containing analogues of BET inhibitors.

Biochemical characterization of BET inhibitors

To evaluate whether the epoxide analogues retained the binding affinity of the unmodified parent compounds to BRD4 bromodomains, we tested their ability to displace acetylated lysine histone 4 peptide from BRD4 bromodomains using an AlphaScreen assay, which mimics the displacement of acetylated H4 lysine from the BRD4 binding site by BET inhibitors. Table 1 demonstrates that the epoxide analogues strongly inhibited the interaction between the tetra-acetylated histone H4 Lys peptide and both individual and tandem dual bromodomains of BRD4 with comparable affinity to the parent compounds.

Table 1. Biochemical characterization of BET inhibitors. IC50s determined by AlphaScreen assay measuring the dose-dependent inhibition of the interaction between BRD4 bromodomains, either single or in tandem, and tetra-acetylated H4 peptide.

Compound number	Average of IC50, μM		
	BRD4(BD1)	BRD4(BD2)	BRD4(BD1BD2)
JQ1	0.06	0.04	0.05
IBET	0.04	0.02	0.04
1 (ZEN-2759)	0.23	0.08	0.28
1A (ZEN-3219)	0.48	0.16	0.47
2 (ZEN-2906)	1.07	0.03	1.41
2A (ZEN-3862)	0.16	0.13	nd
3 (ZEN-3212)	0.02	0.01	0.05
3A (ZEN-3411)	0.05	0.05	0.06

In order to evaluate the direct binding of the compounds to BET proteins, we performed a thermal denaturation protein assay, which measures the increases in protein stability upon compound binding to the protein of interest (Figure 3). We observed that after 30 min incubation the interaction of the non-covalent **2** with BRD4(BD1) resulted in a moderate thermal shift in Tm (ΔTm) of ~ 5 ^{o}C, which is indicative of an increased protein stability upon compound binding (Figure 3, left panel). However, the incubation of BRD4(BD1) with its epoxide analogue, **2A**, resulted in two distinct thermal transitions with ΔTms of 7 ^{o}C and 22 ^{o}C, respectively. If incubation is continued for 4 h, the complex represented by the lower Tm is converted to the higher Tm (Figure 3 right panel). Similar differences in Tm are seen when **1** is compared to **1A** and **3** is compared to **3A** (Figure 3 top and middle panels). Because the lower Tm of **2A** is similar to that of **2,** the data are consistent with a two-step process in which a reversible complex is formed first followed by a reaction that yields an adduct with significantly higher Tm (Figure 3 lower panel). Since the high Tm is higher than that seen with a very potent inhibitor such as **JQ1,**[18] it is very likely a covalent complex. Such two-step binding process was observed for all epoxy-containing BET inhibitors.

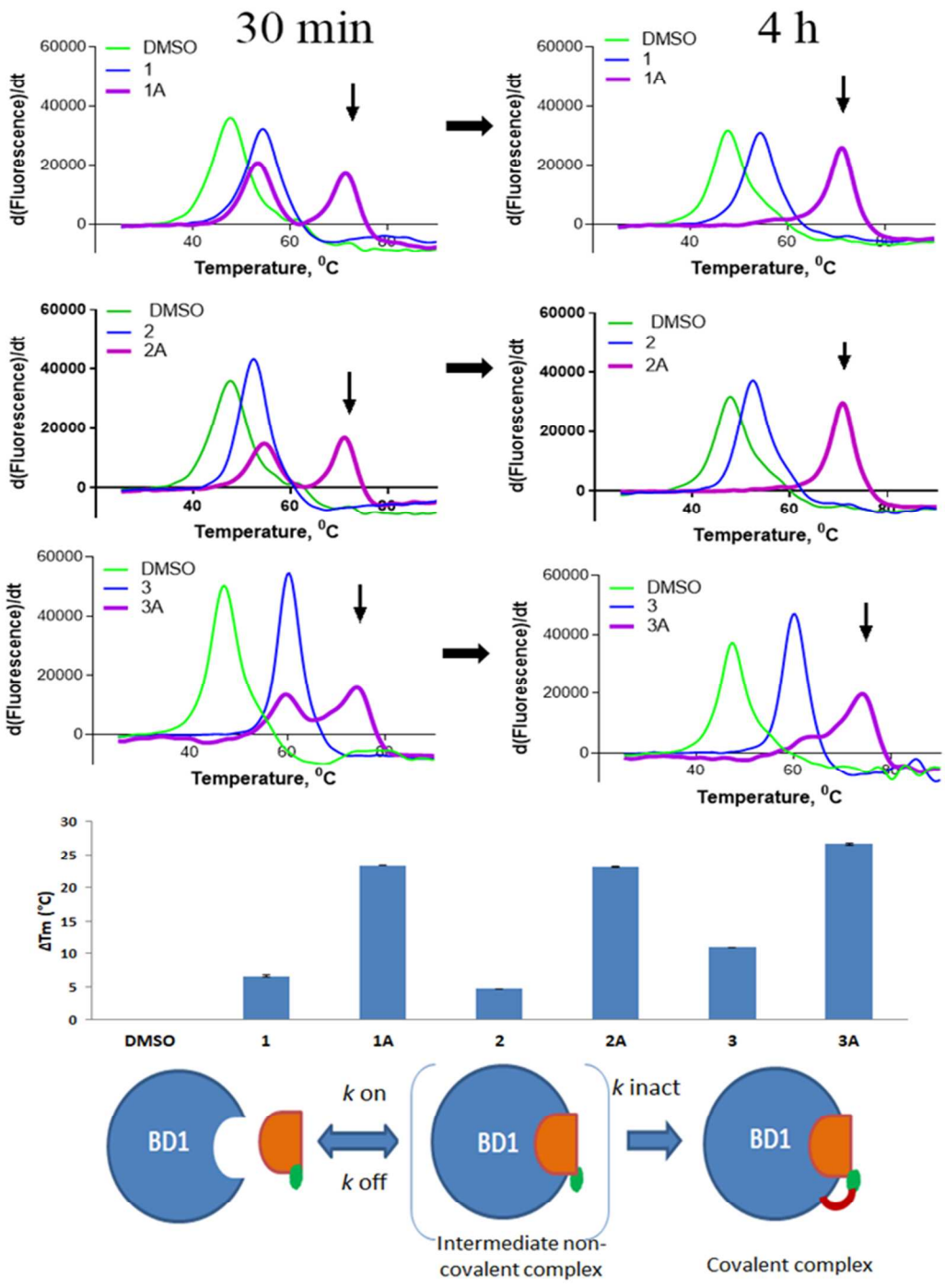

Figure 3. Interaction of BET inhibitors with BRD4(BD1) measured by thermal denaturation assay.

Even though the covalent compounds displayed comparable potencies on BD1 vs. BD2 domains in the AlphaScreen assay, the high Tm shifts were observed with only BD1 domains. Incubations of the covalent compounds with the BD2 domains led to Tm shifts comparable to the parent non-covalent compounds with no higher Tm species forming (Figure S1). Because BD2 contains a Met in a similar position to BD1, this suggests that the presence of Met alone is not a determinant of covalent binding, and additional structural and/or reactivity considerations may play a role. Incubation of covalent compounds or non-covalent controls with several non-BET bromodomains having methionine, cysteine or other amino acid in the corresponding position also demonstrated no high melting Tm species at either 30 min or 4 h, suggesting that the covalent inhibitors are selective for the BET bromodomain family (Figure S2).

To provide further evidence that the third epoxide analogue **3A** bound irreversibly to BRD4(BD1), we monitored its IC50 over time by competitive AlphaScreen assay (Table 2). While the IC50 of its parent **3** did not change over 4 h, consistent with reversible inhibition, the apparent IC50 of **3A** decreased almost 18-fold over 4 h, which is consistent with it making an irreversible, covalent interaction with BRD4(BD1).[19]

Table 2. Time-dependence of biochemical IC50 values of BET inhibitors

Compound number	AlphaScreen (average of IC50, μM)				IC50 fold change
	5 min	30 min	1 h	4 h	
3 (non-covalent)	0.017	0.016	0.008	0.019	1
3A (covalent)	0.274	0.115	0.075	0.015	18

1A Binds Covalently to BRD4(BD1)

To provide definitive evidence that **1A** forms a covalent linkage to BRD4(BD1), we prepared the complex of BRD4(BD1) with **1A** based on the kinetics observed in Figure 3. This complex was stable under various pH conditions (pH=5, 7.4, 9), incubation at room temperature and 37 ^{o}C, and multiple freeze-thaw cycles, as evidenced by retention of the single high Tm peak BRD4 (Figure S3). Similarly, incubation in the presence of excess free methionine or cysteine suggests that the covalent complexes are stable and not reversible (Figure S4).

MALDI-TOF mass spectrometry was conducted on the complex to confirm the covalent complex formation. In addition to a peak corresponding to the mass of unbound BRD4(BD1), we observed a higher mass peak which differed in mass by +325 Da, which is consistent with the formation of a covalent sulfonium linkage as expected from Aferiev et al[17]. (Figure 4). Furthermore, there was a peak with lower mass than BRD4(BD1), suggesting that it results from the loss of a chemical fragment upon ionization in the mass spectrometer. The difference in mass

of 52 Da is consistent with the parent and degradation ions being products from cleavage on either side of the sulfonium ion of the covalent adduct.

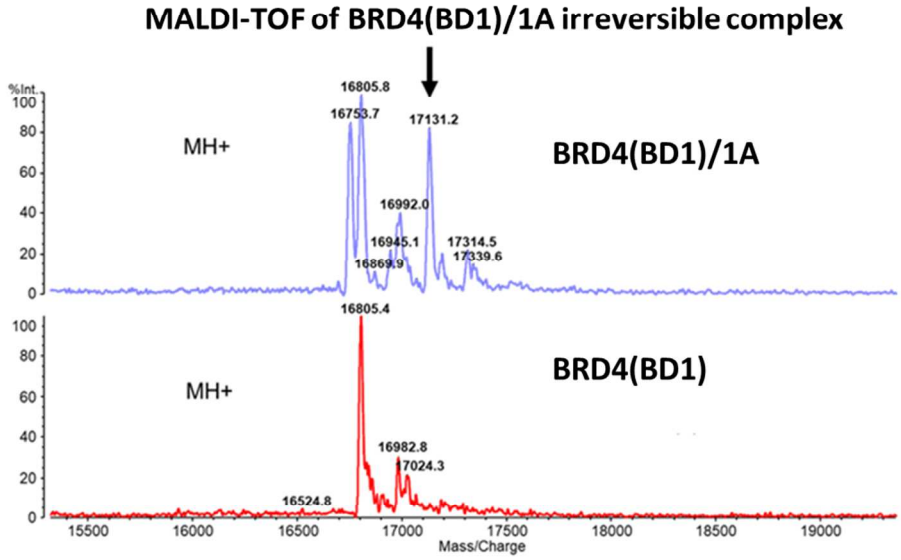

Figure 4. MALDI-TOF spectrometry of **1A**/BRD4(BD1) complex vs. apo BRD4(BD1).

The X-ray co-crystal structure of BRD4(BD1) with **1A** was obtained and resolved at 1.47 Å resolution (Figure 5). **1A** has an epoxide linked to the benzyl's 4-position. The epoxide forms a covalent link with side chain S^{γ} atom of Met149, resulting in a sulfonium ion. The distance between the carbon (named C18) of the isopropanol carbon linker connecting with the Met149 S^{γ} atom is 1.87 Å, which is consistent with a typical sulfur-carbon covalent bond.[17] The S-C covalent bond is elongated by 0.05 Å from the ideal value (1.82 Å), which is well within the range of literature precedents for this type of bond.[19] The electron density around the isopropyl chain (near the covalent bond) clearly indicates that there is only one enantiomeric form of the compound present at the binding pocket. The oxygen substitution off the central pyridone ring forms a water-mediated H-bond with the Lys57 residue side chain and this water molecule

further mediated an interaction with the nitrogen atom of the Gln85 residue side chain amide nitrogen. This scaffold also forms van der Waals interactions with Trp81, Pro82 and Leu92. The dimethyl-isoxazole accepts an H-bond (3.1 Å) from Asn140 amide nitrogen and also forms a water-mediated H-bond to Tyr97 hydroxyl group. This isoxazole ring is positioned between Val87 and Ile146 side chains. The resolved co-crystal structure demonstrates that **1A** binds covalently to Met149 in the binding pocket as predicted. Overall, the co-crystal X-ray structure clearly demonstrates the covalent bond formation between **1A** and S^{γ} atom of Met149 in the BRD4 binding site.

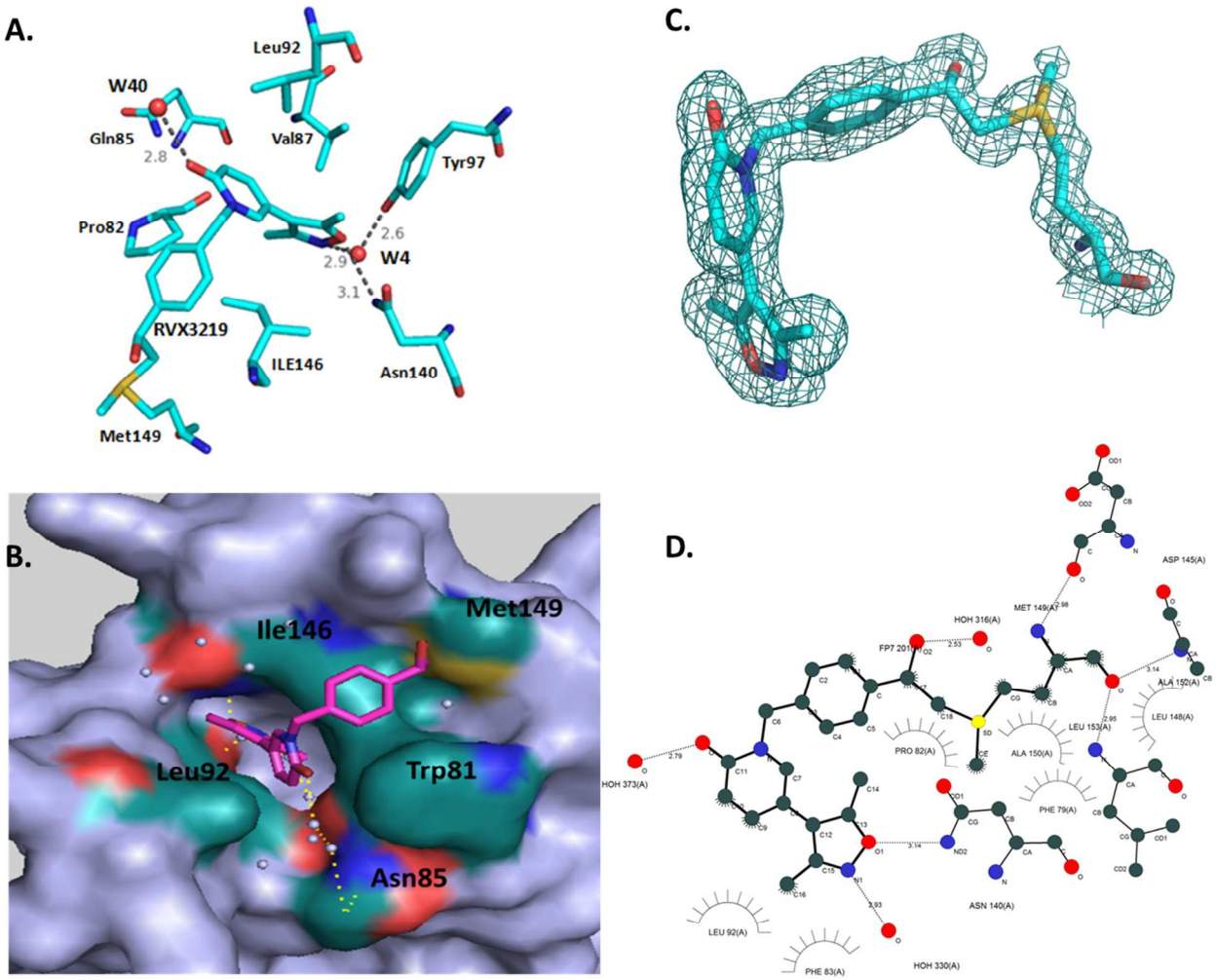

Figure 5. X-RAY co-crystal structure of **1A (ZEN-3219)** with BRD4(BD1), pdb code 6CZU.pdb. A. Interacting amino acid residues of BRD4(BD1) with **1A**. B. Surface representation of **1A** binding mode in BRD4(BD1) binding pocket. C. Electron density map (SigmaA-weighted 2Fo-Fc in teal colour at 1.0 σ contour level) corresponding to compound **1A** bound to BRD4(BD1) and a covalent link between the compound and Sγ atom of Met149. D. Ligand Interaction Diagram (LID) demonstrating the covalent interaction of **1A** and Met149 of BRD4(BD1). Hydrogen bonds are designated with a dashed line and van der Waals interactions are shown by a half "sun" arrangement.

We then overlaid the BRD4(BD1)/**1A** complex with the BRD4(BD1)/**1** complex and observed that the overall orientation of **1A** is shifted in comparison to the parental compound (Figure 6). The anchoring dimethyl-isoxazole ring of **1A** was shifted ~0.7 Å compared to bound **1**. The pyridone ring is also significantly shifted 1.5 Å and rotated by ~17° degrees in the **1A**/BRD4(BD1) complex probably due to the pulling effect of the S-C covalent bond formation. The phenyl ring substituent is also significantly shifted and rotated by 1.6 Å and ~ 2-7 °, respectively. The pulling effect of the covalent bond caused the long range shift in the Trp81, Asp145 and Phe79 residues pulling the amino acid residues to ~1.0 Å, ~0.9 Å and ~1.3 Å away from the compound.

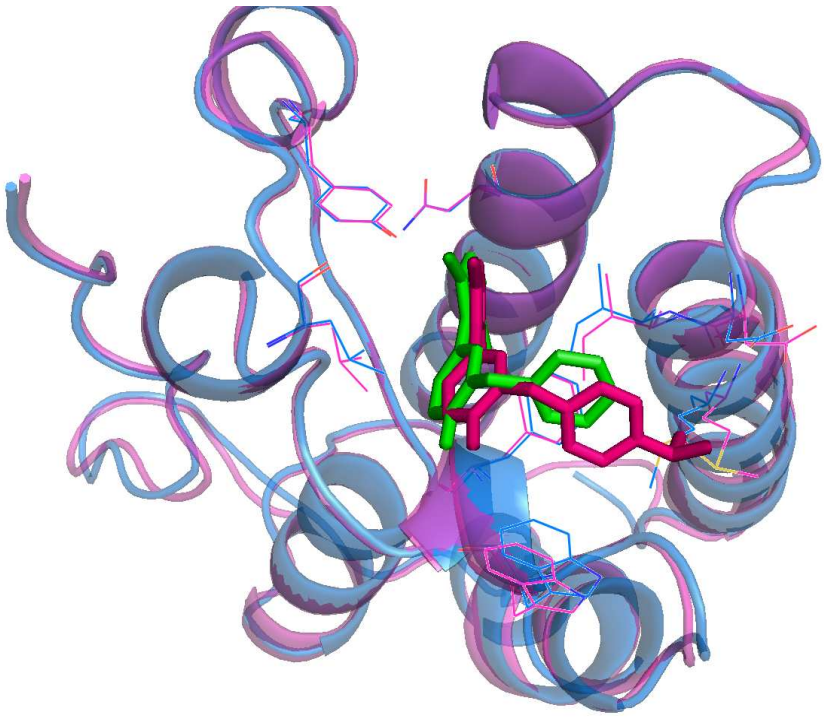

Figure 6. Structural overlay of BRD4(BD1)/**1A** (pink) and **1** (green).

Cellular effects of the covalent inhibition: Sustained effect on proliferation in AML cell line MV4-11

An important benefit of the covalent inhibitors may be an extended inactivation of the protein target, potentially leading to prolonged duration of action and sustained biological effects. This could be mediated by covalently bound BET protein acting in a dominant negative fashion to sequester key transcriptional components which is offset by the speed by which newly synthesized BET protein becomes available to replenish its function after inhibitor is no longer present. To determine whether BET protein had a long half-life to mediate durable inhibition, we determined the half-life of BET proteins by cycloheximide treatment of the acute myeloid leukemia (AML) cell line OCI-AML3 for 3, 6, 24, 48, 72 hours. The estimated half-life of all BET bromodomains was ≥ 48h which is sufficiently long to be able to form a sustained covalent interaction with the irreversible BET inhibitors (Figure S5). To elucidate whether the covalent BET inhibition results in durable anti-proliferative effects, the AML cell line MV4-11 was treated with covalent inhibitor vs. non-covalent control in continuous and washout treatments, respectively (Figure 7). Continuous treatment of either covalent **2A** or non-covalent **2** control showed similar effects on inhibition of proliferation after 48 hours. However, **2A** demonstrated longer durability of anti-proliferative effects in MV4-11 cells when the compound was removed after 24 h and cells incubated for a further 48 h without inhibitor. A similar effect on durability of proliferation was observed with **3A** covalent inhibitor (Figure S6).

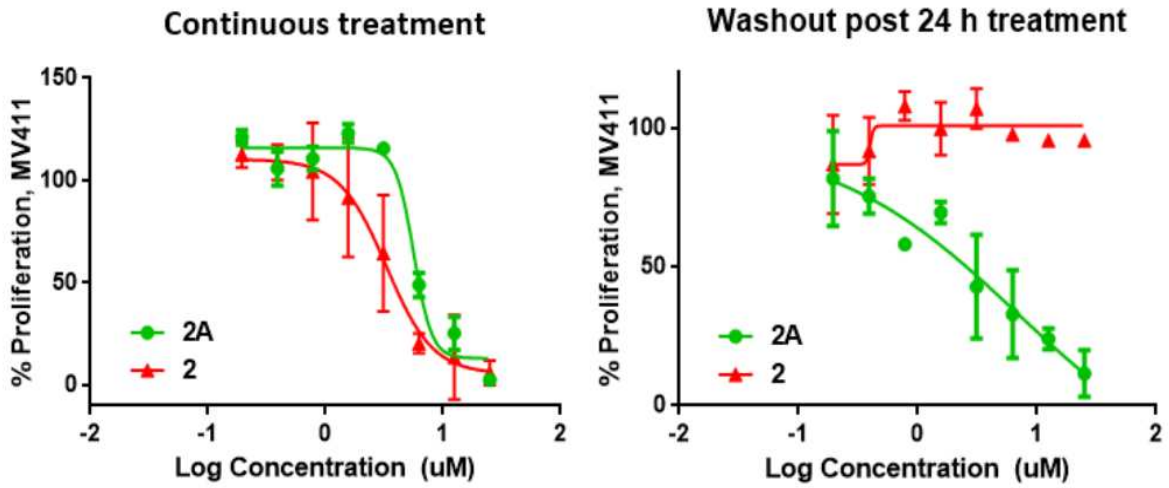

Figure 7. Effect of covalent binding on durability of proliferation in MV4-11 cells. Left panel: Proliferation of MV4-11 was measured after 48 h of continuous treatment with ZEN compounds. Right panel: MV4-11 cell line was treated with **2** (reversible inhibitor) and **2A** (irreversible inhibitor) for 24 h before compounds were removed, replaced with media and proliferation was measured at 48 h.

Next, we then evaluated whether the inhibition of proliferation by a covalent inhibitor and its non-covalent control is due to apoptosis in MV4-11 (Figure 8). Continuous treatment for 72 h with either covalent inhibitor **3A** or its non-covalent control **3** led to the significant induction of apoptosis of 90 and 83%, respectively. In contrast, neither compound had any cytotoxic effect on viability of normal PBMCs (Figure S7).

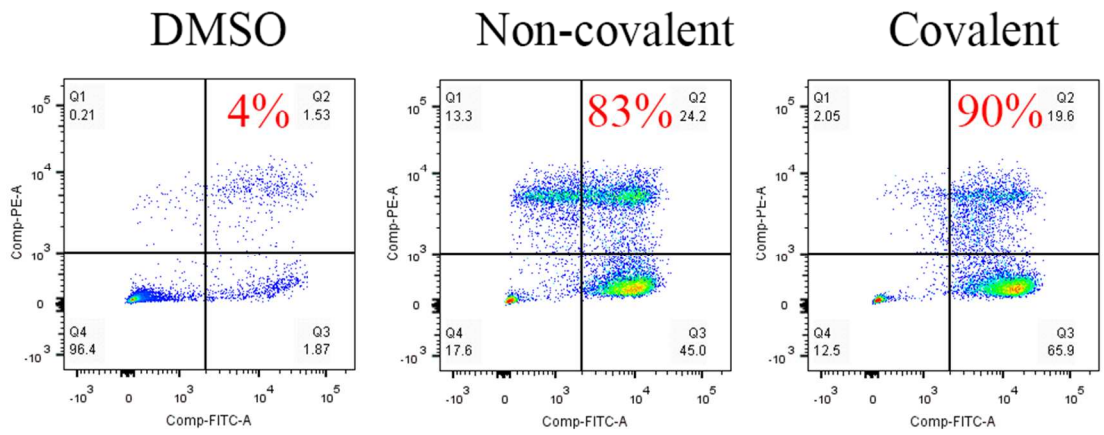

Figure 8. Covalent inhibitor **3A** and its non-covalent analogue **3** induce apoptosis in AML-cell line MV4-11.

Irreversible inhibitor elicits sustained repression of PD markers in hematological cancer cell lines

Furthermore, we evaluated whether the treatment with a covalent inhibitor would lead to sustained repression of previously identified target genes MYC, BCL2, CCR1, GRP183, and IL1RN, which are currently being used to measure target engagement to BET inhibitor ZEN-3694 in the ongoing clinical trial (NCT02711956). We treated MV4-11 for 4 hours with irreversible inhibitor **2A** or with the control compound **2**, after which compounds were removed. Post-washout durability of mRNA repression of MYC, BCL2, CCR1, GRP183, and IL1RN was then time-dependently assessed (Figure 9). **2A** repressed all PD markers significantly longer when compared to the non-covalent **2** control treatment. These data are consistent with **2A** forming an irreversible, covalent linkage with BRD4 in cells.

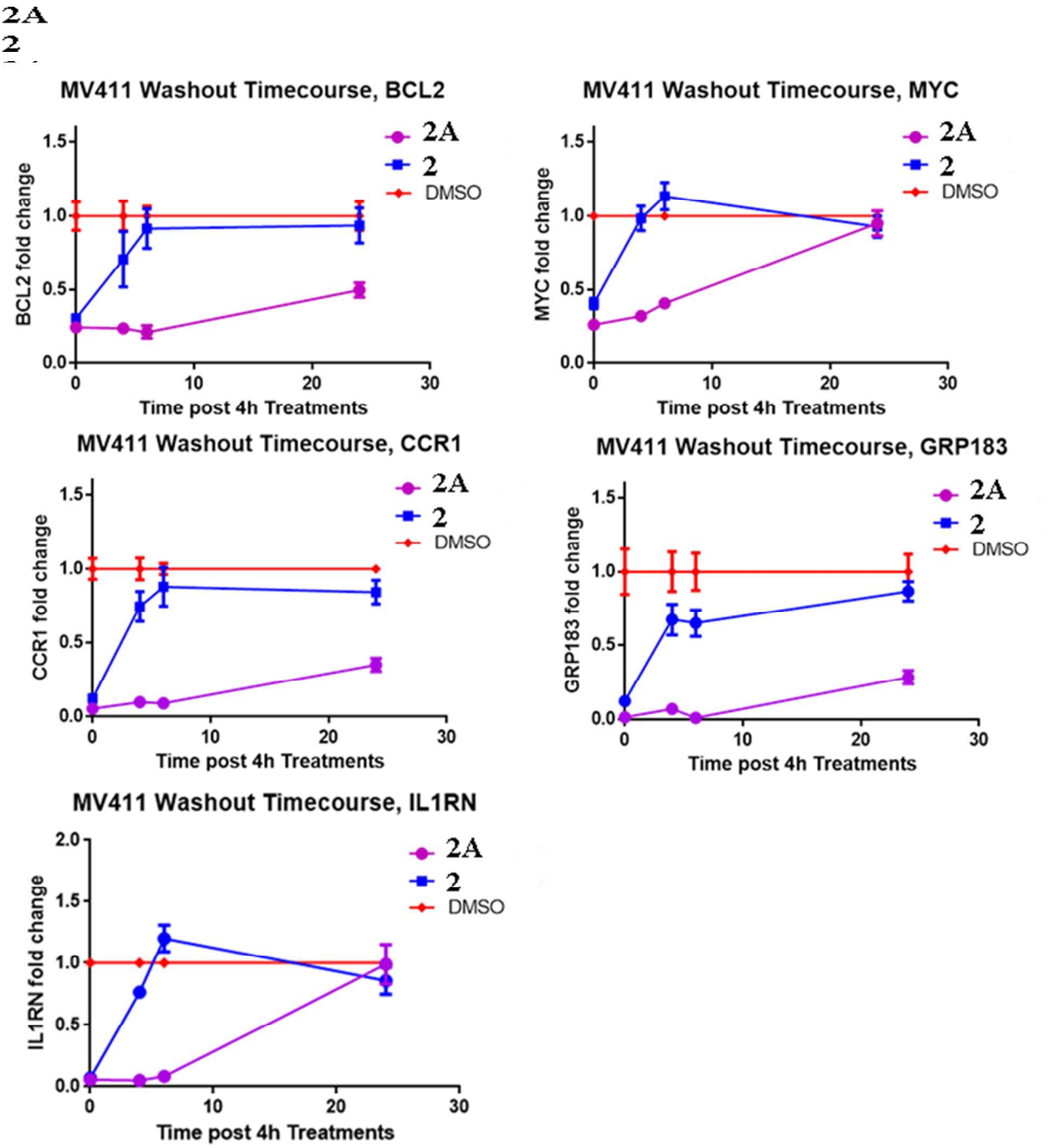

Figure 9. Effect of covalent binding of **2A** on durability of repression of PD markers in a washout time course versus its non-covalent analogue **2.** MV4-11 cells were treated for 4 h with irreversible or reversible inhibitor. After 4 h compounds were removed, cells washed, replaced

with media and cells were harvested at 4, 6 and 24 h post-washout and expression of PD markers was determined.

CONCLUSIONS

Here, we report for the first time the design and characterization of covalent protein inhibitors that target methionine, and illustrate the concept through the design of BET inhibitors that selectively target Met149 in the BRD4(BD1) binding pocket. Lin et al. have recently described a similar approach for enabling methionine bioconjugation using an oxaziridine group, though their approach is not focused on inhibitor design.[21] This covalent interaction was confirmed by thermal shift assay, MALDI-TOF spectrometry and high-resolution X-ray crystal structure of the protein complex. Our findings demonstrate that covalent inhibition leads to durable anti-proliferative effects and decreased mRNA expression of several BET-dependent genes when compared to reversible BET bromodomain inhibitors. Covalent BET inhibitors may offer a novel and potentially superior approach to BET inhibition with long lasting duration of action, durable target modulation, and potential pharmacological effects at lower concentrations in future oncology applications. Targeting methionine may provide an alternative strategy for the design of covalent inhibitors for target evaluation and drug design.

EXPERIMENTAL

1. Synthetic Materials and Methods

Unless otherwise noted, reagents and solvents were used as received from commercial suppliers. Proton nuclear magnetic resonance spectra were obtained on a Bruker ADVANCE 300, 400 or 500 spectrometer. Spectra are given in ppm (δ) and coupling constants, J values, are reported in hertz (Hz). Mass spectra analyses were performed on a Waters Aguity UPLC, Agilent 6130A, Applied Biosystems API-150EX, or a Shimadzu 2020 instrument in ESI or APCI mode when appropriate. The purity of the compounds was analyzed by HPLC, ESI-MS and was >95 %. The HPLC traces for purity are shown in the supplemental information (Figure S8). Molecular Formula Strings are shown in Table S1.

1-Benzyl-5-(3,5-dimethylisoxazol-4-yl)pyridin-2(1H)-one 1 (ZEN-2759).

To a solution of 5-bromo-1,2-dihydropyridin-2-one (150 mg, 0.86 mmol) in acetonitrile (3 mL), benzyl bromide (1.03 mmol) and potassium carbonate (237 mg, 1.72 mmol) was added. The reaction mixture was heated at 80 ^{o}C for 16 h, the reaction mixture was cooled to room temperature, concentrated and purified by chromatography (silica gel, 0–20% ethyl acetate/hexanes) to give 1-benzyl-5-bromo-1,2-dihydropyridin-2-one to which 3,5-dimethyl-4-(4,4,5,5-tetramethyl-1,3,2-dioxaborolan-2-yl)isoxazole (170 mg, 0.76 mmol), 2 M aq. sodium carbonate (0.48 mL, 0.95 mmol) and tetrakis(triphenylphosphine)palladium(0) (37 mg, 0.032 mmol) were added. The reaction mixture was purged with nitrogen and heated at 80 ^{o}C for 16 h, diluted with methylene chloride (30 mL) and washed with brine (2 × 10 mL). The organic layer was dried over sodium sulfate, filtered and concentrated. Purification by chromatography (silica gel, 0–45% ethyl acetate/hexanes) yielded **1** : (120 mg, 43%). ^{1}H NMR (300 MHz, $CDCl_3$) δ

7.31–7.41 (m, 5H); 7.25 (dd, *J* = 2.7, 9.3 Hz, 1H); 7.13 (d, *J* = 2.4 Hz, 1H); 6.76 (d, *J* = 9.3 Hz, 1H); 5.20 (s, 2H); 2.29 (s, 3H); 2.15 (s, 3H); ESI MS *m/z* 281 $[M + H]^+$; HPLC purity: >99%.

5-(3,5-Dimethylisoxazol-4-yl)-1-(2-fluorobenzyl)pyridin-2(1H)-one 2 (ZEN-2906)

To a solution of 5-bromo-1,2-dihydropyridin-2-one (150 mg, 0.86 mmol) in acetonitrile (3 mL), 1-(bromomethyl)-2-fluorobenzene (1.03 mmol) and potassium carbonate (237 mg, 1.72 mmol) was added. The reaction mixture was heated at 80 ^oC for 16 h. The reaction mixture was cooled to room temperature, concentrated and purified by chromatography (silica gel, 0–20% ethyl acetate/hexanes) to give 5-bromo-1-[(2-fluorophenyl)methyl]-1,2-dihydropyridin-2-one (180 mg, 74%) as a white solid: ^1H NMR (300 MHz, DMSO–d_6) δ 8.10 (d, *J* = 2.8 Hz, 1H), 7.58 (dd, *J* = 9.9, 2.8 Hz, 1H), 7.42–7.30 (m, 1H), 7.28–7.08 (m, 3H), 6.42 (d, *J* = 9.7 Hz, 1H), 5.12 (s, 2H). To a solution of 5-bromo-1-[(2-fluorophenyl)methyl]-1,2-dihydropyridin-2-one (0.64 mmol) in 1,4-dioxane (4 mL), 3,5-dimethyl-4-(4,4,5,5-tetramethyl-1,3,2-dioxaborolan-2-yl)isoxazole (170 mg, 0.76 mmol), 2 M aq. sodium carbonate (0.48 mL, 0.95 mmol) and tetrakis(triphenylphosphine)palladium(0) (37 mg, 0.032 mmol) were added. The reaction mixture was purged with nitrogen and heated at 80 ^oC for 16 h. The mixture was diluted with methylene chloride (30 mL) and washed with brine (2 × 10 mL). The organic layer was dried over sodium sulfate, filtered and concentrated.

Purification by chromatography (silica gel, 0–45% ethyl acetate/hexanes) yielded **2** (48 mg, 25%) as a white solid: ^1H NMR (300 MHz, DMSO–d_6) δ 7.96 (d, *J* = 2.1 Hz, 1H), 7.52 (dd, *J1* = 6.6 Hz, J2 = 2.7 Hz, 1H), 7.46–7.36 (m, 1H), 7.24–7.06 (m, 3H), 7.96 (d, *J* = 2.1 Hz, 1H), 5.14 (s, 2H), 2.36 (s, 3H), 2.19 (s, 3H); ESI *m/z* 299 $[M + H]^+$; HPLC purity: >99%

1-Benzyl-6-(3,5-dimethylisoxazol-4-yl)-lH-benzo[d]imidazol-4-amine 3 (ZEN-3212)

A mixture of 6-bromo-1H-1,3-benzodiazol-4-amine (1.0 g, 4.7 mmol), 3,5-dimehyl-4-(4,4,5,5-tetramethyl-1,3,2-dioxaborolan-2-yl)-1,2-oxazole (4.5 g, 6.6 mmol), K_2CO_3 (1.3 g, 9.4 mmol), 1,4-dioxane (48 mL) and water (3.5 mL) was degassed with nitrogen for 20 minutes followed by addition of tetrakis (tri-phenylphosphine)palladium(0) (550 mg, 0.94 mmol). The mixture was heated at 90 °C for 18 hours then cooled to room temperature. The crude reaction mixture was purified by chromatography (silica gel, 0–10% methanol/dichloromethane) to obtain 6-(3,5-dimethylisoxazol-4-yl)-1H-benzo[d] imidazol-4-amine (760 mg, 68%) as an off-white solid: ^{1}H NMR (500 MHz, $CDCl_3$) δ 7.98 (s, 1H), 6.74 (s, 1H), 6.40 (s, 1H), 4.45 (s, 2H), 2.38 (s, 3H), 2.25 (s, 3H); ESI *m/z* 229 $[M + H]^+$.

To a solution of 6-(3,5-dimethylisoxazol-4-yl)-1H-benzo[d] imid-azol-4-amine (290 mg, 1.27 mmol) in CH_3CN (15 mL), potassium carbonate (350 mg, 2.54 mmol) and benzyl chloride (200 mg, 1.59 mmol) were added. The reaction mixture was stirred at 60 °C for 16 h. The mixture was diluted with methylene chloride (20 mL) and filtered through a layer of Celite. The filtrate was concentrated and purified by chromatography (silica gel, 0-10% CH_3OH/CH_2Cl_2) to obtain **3** (109 mg, 27%) as an off-white solid: ^{1}H NMR (300 MHz, $CDCl_3$) δ 7.95 (s, 1H), 7.37-7.34 (m, 3H), 7.23-7.20 (m, 2H), 6.46 (d, J = 1.2 Hz, 1H), 6.40 (d, J = 1.2 Hz, 1H), 5.34 (s, 2H), 2.31 (s, 3H), 2.16 (s, 3H); ESI MS *m/z* 319 $[M + H]^+$; HPLC purity: >99%

5-(Dimethyl-1,2-oxazol-4-yl)-1-{[4-(oxiran-2-yl)phenyl]methyl}-1,2-dihydropyridin-2-one 1A (ZEN-3219)

A mixture of compound of 5-(3,5-dimethylisoxazol-4-yl)pyridin-2(1H)-one (100 mg, 0.49 mmol), 2-(4-(chloromethyl)phenyl) oxirane (90 mg, 0.54 mmol) and K_2CO_3 (135 mg, 0.98 mmol) in CH_3CN (6 mL) was stirred at 70 °C for 16 h. The reaction mixture was allowed to cool

to room temperature and was filtered through a layer of Celite. The filtrate was concentrated and purified on silica gel to obtain the desired product **1A** as an off-white solid (94 mg, 57%). ^{1}H NMR (300 MHz, $CDCl_3$) δ 7.40–7.12 (m, 6H), 6.64 (d, J = 9.3 Hz, 1H), 5.17 (s, 2H), 3.85–3.84 (m, 1H), 3.16–3.13 (m, 1H), 2.78–2.74 (m, 1H), 2.30 (s, 3H), 2.15 (s, 3H); ESI MS *m/z* 323 $[M + H]^+$; HPLC purity: >99%.

6-(Dimethyl-1,2-oxazol-4-yl)-1-{[4-(oxiran-2-yl)phenyl]methyl}-1H-1,3-benzodiazol-4-amine 3A (ZEN-3411)

A mixture of 6-bromo-1H-1,3 benzodiazol-4-amine (1.0 g, 4.7 mmol), 3,5-dimehyl-4-(4,4,5,5-tetramethyl-1,3,2-dioxaborolan-2-yl)-1,2-oxazole (4.5 g, 6.6 mmol), K_2CO_3 (1.3 g, 9.4 mmol), 1,4-dioxane (48 mL) and water (3.5 mL) was degassed with nitrogen for 20 minutes followed by addition of tetrakis (tri-phenylphosphine) palladium(0) (550 mg, 0.94 mmol). The mixture was heated at 90 °C for 18 hours then cooled to room temperature. The crude reaction mixture was purified by chromatography (silica gel, 0–10% methanol/dichloromethane) to obtain 6-bromo-1H-1,3 benzodiazol-4-amine 6-(3,5-dimethyl-1,2 –oxazol-4-yl)-1H-1,3-benzodiazol-4-amine (760 mg, 68%) as an off-white solid: ^{1}H NMR (500 MHz, $CDCl_3$) δ 7.98 (s, 1H), 6.74 (s, 1H), 6.40 (s, 1H), 4.45 (s, 2H), 2.38 (s, 3H), 2.25 (s, 3H); ESI *m/z* 229 $[M + H]^+$. To a solution of 6-(3,5-dimethylisoxazol-4-yl)-1H-benzo[d] imidazol-4-amine (100 mg, 0.44 mmol) in CH_3CN (5 mL) was added potassium carbonate (121 mg, 0.88 mmol) and 2-(4-(chloromethyl)phenyl) oxirane (81 mg, 0.48 mmol). The reaction mixture was stirred at 60 °C for 16 h. The mixture was diluted with methylene chloride (20 mL) and filtered through a layer of Celite. The filtrate was concentrated and purified by chromatography (silica gel, 0–10% CH_3OH/CH_2Cl_2) followed by reverse phase comiflash to obtain **3A** (70 mg, 44%) as an off-white solid: ^{1}H NMR (300 MHz, CD_3OD) δ 8.18 (s, 1H), 7.27 (s, 4H), 6.55 (d, J = 1.2 Hz, 1H), 6.45 (d, J = 1.5 Hz, 1H),

5.44 (s, 2H), 3.84 (dd, J = 4.2, 2.7 Hz, 1H), 3.09 (dd, J = 5.4, 4.2 Hz, 1H), 2.74 (dd, J = 5.4, 2.7 Hz, 1H), 2.24 (s, 3H), 2.14 (s, 3H); ESI MS m/z 361 $[M + H]^+$; HPLC purity: 97.3%.

5-(Dimethyl-1,2-oxazol-4-yl)-1-(3-fluoro-4-(oxiran-2-yl)benzyl)pyridin-2(1H)-one 2A

(ZEN-3862)

A reaction mixture of (4-bromo-3-fluorophenyl)methanol (500 mg, 2.44 mmol), pyridine (578 mg, 7.32 mmol) and MsCl (559 mg, 4.88 mmol) in CH_2Cl_2 (10 mL) was stirred at rt for 16 h. The reaction mixture was diluted with CH_2Cl_2, and it was filtered through a layer of Celite. The filtrate was concentrated to give 1-bromo-4-(chloromethyl)-2-fluorobenzene as an off-white solid (4.2 g, 95%): ^{1}H NMR (500 MHz, $CDCl_3$) δ 7.63–7.43 (m, 3H), 6.31 (s, 2H). A mixture of 5-(3,5-dimethylisoxazol-4-yl)pyridin-2(1H)-one (285 mg, 1.5 mmol) which was prepared according to literature procedure (WO 2014096965, compound 14[21]), 1-bromo-4-(chloromethyl)-2-fluorobenzene (368 mg, 1.65 mmol) and K_2CO_3 (414 mg, 3.0 mmol) in CH_3CN (10 mL) was stirred at 70 °C for 16 h. The reaction mixture was allowed to cool to room temperature and filtered through a layer of Celite. The filtrate was concentrated and purified on silica gel to obtain 1-[(4-bromo-3-fluorophenyl)methyl]-5-(3,5-dimethyl-1,2-oxazol-4-yl-1,2-dihydropyridin-2-one as an off-white solid (180 mg, 32%). ^{1}H NMR (300 MHz, $CDCl_3$) δ 7.59–7.54 (m, 1H), 7.30–7.26 (m, 2H), 7.17–7.12 (m, 2H), 7.03 (d, J = 8.1 Hz, 1H), 5.14 (s, 2H), 2.36 (s, 3H), 2.22 (s, 3H); ESI MS m/z 378 $[M + H]^+$. To a solution of 1-[(4-bromo-3-fluorophenyl)methyl]-5-(3,5-dimethyl-1,2-oxa-zol-4-yl-1,2-dihydropyridin-2-one (180 mg, 0.48 mmol) in DMF (5 mL) was added tributyl(vinyl)stannane (197 mg, 0.62 mmol) and $Pd(PPh_3)_2Cl_2$ (34 mg, 0.048 mmol). The reaction mixture was purged with nitrogen and heated at 85 °C for 16 h. The mixture was filtered through a layer of Celite. The filtrate was concentrated.

Purification by chromatography (silica gel, 0–40% ethyl acetate/dichloromethane) left 5-(3,5-dimethyl-1,2-oxazol-4-yl)-1-[(4-ethenyl-3-fluorophenyl)methyl]-1,2-dihydropyridin-2-one (83 mg, 53%) as an orange oil: ^{1}H NMR (300 MHz, $CDCl_3$) δ 7.51–7.46 (m, 1H), 7.26–7.25 (m, 1H), 7.14 (d, J = 1.8 Hz, 1H), 7.09–7.00 (m, 2H), 6.91–6.74 (m, 2H), 5.82 (d, J = 17.7 Hz, 1H), 5.40 (d, J = 11.1 Hz, 1H), 5.15 (s, 2H), 2.32 (s, 3H), 2.18 (s, 3H); ESI MS *m/z* 325 $[M + H]^+$. 5-(3,5-dimethyl-1,2-oxazol-4-yl)-1-[(4-ethenyl-3-fluorophenyl)methyl]-1,2- dihydro-pyridin-2-one was dissolved in acetone (3 mL) and water (1 mL) at 0 °C and combined with NBS (50 mg, 0.29 mmol). The reaction mixture was stirred at rt for 6 h. To the mixture above at 0 °C, NaOH (21 mg, 0.52 mmol) was added and the mixture was stirred at rt for 16 h. The reaction mixture was filtered through a layer of Celite. The filtrate was concentrated. Purification by chromatography (silica gel, 0–40% ethyl acetate/dichloromethane) left 5-(dimethyl-1,2-oxazol-4-yl)-1-(3-fluoro-4-(oxiran-2-yl)benzyl) pyridin-2(1H)-one (53 mg, 60%) as an off-white solid. ^{1}H NMR (500 MHz, DMSO–d_6) δ 7.94 (d, J = 2.5 Hz, 1H), 7.50 (dd, J = 9.0, 2.5 Hz, 1H), 7.24 (d, J = 11.5 Hz, 1H), 7.19–7.17 (m, 2H), 6.51 (d, J = 9.0 Hz, 1H), 5.12 (s, 2H), 4.08 (dd, J = 4.0, 2.5 Hz, 1H), 3.14 (dd, J = 5.5, 4.0 Hz, 1H), 2.87 (dd, J = 5.5, 2.5 Hz, 1H), 2.36 (s, 3H), 2.19 (s, 3H); ESI *m/z* 341 $[M + H]^+$; HPLC purity: 98.1%.

2. AlphaScreen

Single and dual bromodomain constructs with an N-terminal His-tag were cloned, expressed, and purified by nickel affinity and size-exclusion chromatography by Genscript or Xtal BioStructures. Fractions representing monomeric protein were pooled and frozen at -80 °C for use in subsequent experiments. The AlphaScreen® Histidine (Nickel Chelate) Detection Kit (Perkin Elmer, 6760619M) containing 1 mL of Streptavidin Donor Beads, 1 mL of Nickel Chelate Acceptor Beads, and 1.5 mL of 10X Buffer was used according to the manufacturer's

instructions. Briefly, N-terminally His-tagged single and dual bromodomains (20-200 nM) and biotinylated tetra-acetylated histone H4 peptide (3-75 nM) (Millipore 12-379) were mixed in 50 mM HEPES, 100 mM NaCl, and 0.1% bovine serum albumin buffer, pH 7.4, under green light. Nickel chelate acceptor beads and streptavidin donor beads were added to a final concentration of 2 μg/mL. Serially diluted compounds were added to the reaction mixture in a white 96 well plate (Greiner). After 30 min incubation at room temperature, luminescence was measured at 570 nm by a SynergyH4 plate reader (Biotek). IC50 values were determined from a dose response curve.

3. Protein Thermal Denaturation Assay

Binding of purified N-terminally His-tagged recombinant BRD4(BD1) to ZEN inhibitors was investigated using the protein thermal shift assay (PTS™, Life Technologies). 5 μM of bromo-domains were incubated with 100 μM of the irreversible inhibitors or the control compounds in the presence of 5X SYPRO orange protein stain (Life Technologies S-6650) for 30 min or 4 hours in 50 mM NaCl/ 50 mM HEPES buffer, pH 7.4. Melting temperatures (Tm) were calculated using Applied Biosystems Protein Thermal Shift™ Software v1.1.

4. MALDI-TOF characterization

Analyses were performed on a Shimadzu Biotech Axima TOF2 (Shimadzu Instruments) matrix-assisted-laser desorption/ ionization Time-of-Flight (MALDI-TOF) mass spectrometer. Proteins were analyzed in positive ion Linear mode. For intact protein mass measurement the instrument was set with a mass range extending to 50 kd using a pulsed extraction setting of 16952. Apomyoglobin MH+ of 16952 and MH2+ of 8476 were used as the standard to calibrate the instrument. A 0.5 μL aliquot was applied to the MALDI target followed by the addition of 0.5

μL of Sinapinic acid as the desorption matrix (10 mg/mL in 0.1% TFA: Acetonitrile 50:50) followed by air drying prior to insertion into the vacuum source.

5. X-ray Crystallography

The complex with **1** (**ZEN-2759)** was prepared by adding 2 mM **1** to 1 mg/mL BRD4(BD1)(BRD4 amino acids 44-170). The mixture was incubated for 30 minutes at room temperature; concentrated to 7 mg/mL; and setup with broad formulation screens using the sitting drop vapor diffusion method. Co-crystals grew to usable size in three days using 0.2 M potassium fluoride and 8% (W/V) PEG 3350 as reservoir formulation. To generate BRD4-(BD1)/**1A** co-crystals, **1A** (100 mM stock in 100% DMSO) was added to 1 mg/mL BRD4(BD1) with gentle mixing to achieve a final concentration of 0.33 mM **1A**, resulting in a compound:protein ratio of 5:1. The BRD4(BD1)/inhibitor complex was incubated at room temperature for 4 hours to form an covalent adduct and then concentrated up to 3.0-4.0 mg/mL using the 3 kDa cut-off Centricon concentrator. This complex was crystallized using the sitting drop vapor diffusion method at room temperature. The screening process yielded several crystallization conditions that produced crystals of sufficient size and grew to a maximum size after three days. The crystallization condition that resulted in the crystal selected for X-ray diffraction data collection was obtained from a well solution of 0.2 M Ammonium Sulfate, 0.1 M Bis-Tris pH 6.5, 25% PEG 3350. Co-crystals of both complexes were harvested, treated with the crystallization solution supplemented with 20-27% ethylene glycol and flash frozen in liquid nitrogen. X-ray diffraction data were measured at Beamline X29A, NSLS synchrotron facility, Brookhaven National Laboratory. The X-ray diffraction data were reduced using HKL2000 (Otwinowski and Minor, 1997) (Supplementary Table S2). The crystal structures were solved by molecular replacement with Molrep. Model building and refinement were pursued using COOT

(Emsley, 2004) and REFMAC (Vagin, 2004), respectively. Inspection of the initial electron density maps showed unambiguous compound density in each of the two structures. **1** was modeled in with the protein and refined to a resolution of 1.88 Å with Rfactor and Rfree of 16.2% and 22.6%, respectively and good stereochemistry (Supplementary data Table S2). In the other structure initial electron density map, **1A** epoxide was observed as a linearized, covalent adduct to Met149. Initial model building and refinement were done with neither of Met149 nor this compound in the structure. After placement of the solvent molecules, Met149 and **1A** compound were modeled and refined. A residual element of density linked to the sulfur linker atom was modeled as a methyl, but this group could not be unambiguously assigned. The co-structure was further refined to a resolution of 1.47 Å with Rfactor and Rfree of 14.5% and 19.4%, respectively and good stereochemistry (Supplementary Table S3).

6. Proliferation assay

The MV4-11 cell line was obtained from ATCC and propagated according to manufacturer's instructions. Cells were counted using a Countess automated cell counter (Life Technologies) and seeded in 96 well plates between 25,000 and 50,000 cells/well. Two-fold dilutions of covalent inhibitors vs. non-covalent controls were added in triplicate wells and compounds were added at the time of seeding. DMSO at a final concentration of 0.1% was used as a negative control. Compounds and cells were incubated for 72 hours at 37 °C, 5% CO_2. Twenty microliters of the CellTiter 96 Aqueous One Solution Reagent (Promega) were then added to each well, and the cells were incubated at 37 °C, 5% CO_2 for three hours. Absorbance at 490 nm was read on a MultiSkan GO plate reader (Thermo Scientific) using the precision measurement mode. The percentage of proliferation was calculated as follows: [(ODSample-ODblank)/OD DMSO]*100. Determination of the IC50 values was done with the GraphPad Prism software. In the washout

proliferation studies cells were plated in 96 well plates at 25,000 cells/well. Two fold dilutions of the compounds were added in triplicate wells in the beginning of treatments. In the washout study cells were treated for 24 hours, then the compounds were removed, cells washed twice with the conditioned media, and left to proliferate in the compound-free media for 48 hours after which the proliferation was measured using CellTiter 96 Aqueous One Solution Reagent (Promega) kit. In the corresponding continuous studies cells were plated and treated as described above and proliferation was measured after 48 or 72 h of continuous treatments.

7. Gene expression analysis and washouts

Covalent inhibitors and the corresponding non-covalent control compounds was transferred to media (IMDM+ 10% FBS) at a final concentration of 0.2% DMSO. Media containing 0.2% DMSO alone was used as a control. Cells were counted and plated in 96 well u-bottom plates at a density of 50,000 cells per well in 50 µL. An equal volume of media containing either compound or DMSO was added to appropriate wells and plates were incubated for 4 h at 37 ºC, 5% CO2. Immediately prior to harvesting the cells, 2X cell lysis solution was prepared from components of the mRNA Capture PLUS kit (Life Technologies) according to the manufacturer's instructions. Cells were pelleted by centrifugation at 1000 rpm for five minutes, 60 µL of supernatant was carefully removed so as not to disturb the pellet and 45 µL of 2X Lysis buffer was added directly to each well and incubated for five min at room temperature to allow for complete cell lysis. The contents of the wells were mixed briefly, transferred to the mRNA Catcher PLUS plate and incubated for 1 h at room temperature. Plates were washed three times with 100 µL of Wash Buffer (W15), eluted with 70 µL of Elution Buffer (E3) for 5 min at 68 ºC in a PCR machine, and immediately place on ice. Real-time PCR reactions using the components of RNA UltraSense One-Step qRT-PCR System (Life Technologies, 11732927) were used along

with Taqman primer probes and Cyclophilin A in a final volume of 8 μL per well master mix and 2 μL per well of RNA. One-step real-time PCR reactions were run on a ViiA™7 Real-Time PCR machine using standard conditions and analyzed using Applied Biosystems software. Results were plotted as a percentage of the DMSO-treated control. In the washout studies cells were treated with the covalent vs. non-covalent control continuously for 4 hours, then replaced with the compound-free media after washing 3 times with the conditioned media. After 0, 4, and 24 hours post washout cells were harvested as described above, and samples were processed using Life Technologies mRNA Catcher kit and Ultrasense kit reagents.

8. Flow cytometry

MV4-11 cells were seeded at 5 x 10^6 cells/2 mL in 6 well plates. Cells were treated continuously for 72 h with **3** and **3A**. After, cells were stained with FITC Annexin V Apoptosis Detection Kit according to manufacturer (BD Pharmingen) and immediately analyzed with a BD LSRII flow cytometer. Data was analyzed and dot plots were made using FlowJo software.

ASSOCIATED CONTENT

ANCILLARY INFORMATION

Supporting information: The following files are available free of charge. Biochemical characterization of the stability of the covalent complexes, selectivity of the covalent compounds towards non-BET bromodomain proteins and BRD4(BD2) bromodomain; SMILES, HPLC traces of the active compounds, X ray data reduction statistic and crystal parameters, crystallographic refinement.

X-ray crystal structure refinement data is available free of charge via the Internet at http://pubs.acs.org.

PDB ID Codes: Coordinate have been deposited in the PDB accession code 6CZU.pdb for **1A** (**ZEN-3219)** and 6CZV.pdb for **1** (**ZEN-2759)**

Authors will release the atomic coordinates and experimental data upon article publication

AUTHOR INFORMATION

Corresponding Author

Corresponding Author Information: Olesya A. Kharenko, Olesya@zenithepigenetics.com

Present Addresses

Kevin G. McLure, Vitrisa Therapeutics, 700 Larkspur Landing Circle, Suite 199, Larkspur, CA 94939.

Peter R. Young, LAM Therapeutics, 530 Old Whitfield Street, Guilford CT 06437.

Bryan C. Duffy NYS DOH Wadsworth Center Biggs Laboratory, Wadsworth Center, NYS Dept. of Health, Empire State Plaza, PO Box 509, Albany, NY 12201 USA, bryan.duffy@health.ny.gov

Author Contributions

The manuscript was written through contributions of all authors. All authors have given approval to the final version of the manuscript.

Funding Sources

This work was funded by Zenith Epigenetics Ltd.

ACKNOWLEDGEMENTS

We thank the AMRI team for compound synthesis

ABBREVIATIONS

PROTAC, proteolysis-targeting chimera, BET, Bromodomain and Extra-Terminal protein, MALDI-TOF, matrix assisted laser desorption ionization-time of flight mass spectrometry

REFERENCES

(1) Filippakopoulos, P.; Knapp, S. The bromodomain interaction module. *FEBS Lett*. **2012**, 17, 586, 2692-2704.

(2) Filippakopoulos, P.; Knapp, S. Targeting bromodomains: epigenetic readers of lysine acetylation. *Nat. Rev. Drug. Discov*. **2014**, 13, 337-356.

(3) Doroshow, D. B.; Eder, J. P.; LoRusso, P. M. BET inhibitors: a novel epigenetic approach. *Ann. Oncol.* **2017**, 28, 1776–1787.

(4) Shi, J.; Vakoc, C. R. The mechanisms behind the therapeutic activity of BET bromodomain inhibition. *Mol. Cell* **2014**, 54 (5), 728-736.

(5) Kharenko, O. A.; Hansen, H. C. Novel approaches for targeting BRD4. *Drug Discovery Today: Technologies*. **2017**, 24, 19-24.

(6) Chan, K.-H.; Zengerle, M.; Testa, A.; Ciulli, A. Impact of target warhead and linkage vector on inducing protein degradation: comparison of bromodomain and extra-terminal (BET) degraders derived from triazolodiazepine (JQ1) and tetrahydroquinoline (I-BET726) BET inhibitor scaffolds. *J. Med. Chem*. **2018**, 61, 504-513.

(7) Lu, J.; Qian, Y.; Altieri, M.; Dong, H.; Wang, J.; Raina, K.; Hines, J.; Winkler, J. D.; Crew, A. P.; Coleman, K.; Crews, C. M. Hijacking the E3 ubiquitin ligase cereblon to efficiently target BRD4. *Chem. Biol*. **2015**, 22, 755-763.

(8) Raina, K.; Lu, J.; Qian, Y.; Altieri, M.; Gordon, D.; Rossi, A. M.; Wang, J.; Chen, X.; Dong, H.; Siu, K.; Winkler, J. D.; Crew, A. P.; Crews, C. M.; Coleman, K. G. Selective small molecule induced degradation of the BET bromodomain protein BRD4. *Proc. Natl. Acad. Sci. USA* **2016**, 113, 7124-7129.

(9) Zengerle, M.; Chan, K. H.; Ciulli, A. Selective small molecule induced degradation of the BET bromodomain protein BRD4. *ACS Chem. Biol.* **2015**, 10, 1770-1777.

(10) Winter, G. E; Buckley, D. L; Paulk, J.; Roberts, J. M.; Souza, A.; DhePaganon, S,; Bradner, J. E. Phthalimide conjugation as a strategy for in vivo target protein degradation. *Science* **2015**, 348, 6241, 1376-1381.

(11) Zhong, H-J.; Lu, L.; Wong, C. L.; Peng, C.; Yan, S-C.; Ma, D-L.; Cai, Z.; Wang, H. An iridium(III)-based irreversible protein–protein interaction inhibitor of BRD4 as a potent anticancer agent *Chem. Sci*., **2015**, 6, 5400-5408.

(12) Singh, J.; Petter, R. C.; Baillie, T.A.; Whitty, A. The resurgence of covalent drugs. *Nat Rev Drug Discov*. **2011**, 10, 307–317.

(13) Lagoutte, R.; Patouret, R., Winssinger, N. Covalent inhibitors: an opportunity for rational target selectivity. **2017,** Curr. Opin. Chem. Biol. 39, 54-63.

(14) Davids, M. S.; Brown, J. R. Ibrutinib: a first in class covalent inhibitor of Bruton's tyrosine kinase. *Future Oncol*. **2014**, 10, 957-967.

(15) Bauer R. A. Covalent inhibitors in drug discovery: from accidental discoveries to avoided liabilities and designed therapies. *Drug Discovery Today*, **2015**, 20, 1061-1073.

(16) Daguer, J. P.; Zambaldo, C.; Abegg, D.; Barluenga, S.; Tallant, C.; Muller, S.; Adibekian, A.; Winssinger, N. Identification of covalent bromodomain binders through DNA display of small molecules *Angew. Chem. Int. Ed.* **2015**, 54, 1-6.

(17) Alferiev, I. S.; Hinson, J. T,; Ogle, M., Breuer, E, Levy R. J., High reactivity of alkyl sulfides towards epoxides under conditions of collagen fixation – a convenient approach to 2-amino-4-butyrolactones. *Biomaterials*, **2001**, 18, 2501-2506.

(18) McLure, K. G.; Gesner, E. M.; Tsujikawa, L.; Kharenko, O. A.; Attwell, S.; Campeau, E.; Wasiak, S.; Stein, A.; White, A.; Fontano, E.; Suto, R. K.; Wong, N. C.; Wagner, G. S.; Hansen, H. C.; Young, P. R. RVX-208, an inducer of ApoA-I in humans, is a BET bromodomain antagonist. *PloS one, Public Library of Science*, **2013**, 8, 1-12.

(19) Yang, J.; Copeland, R. A.; Lai, Z. Defining balanced conditions for inhibitor screening assays that target bisubstrate enzymes. *J Biomolecular Screening*, **2009**, 14, 111-120.

(20) Allen, F. H.; Kennard, O.; Watson, D. G.; Tables of bond lengths determined by X-ray and neutron diffraction. Part 1. Bond lengths in organic compounds. *J. Chem.Soc.Perkin Trans. II.* 1987, S1-S19.

(21) Lin, S.; Yang, X.; Jia, S.; Weeks, A. M.; Hornsby, M.; Lee, P. S.; Nichiporuk, R. V.; Iavarone, A. T.; Wells, J. A.; F. Dean Toste, F. D.; Chang, C. J. Redox-based reagents for chemoselective methionine bioconjugation. *Science*, 2017, 335, 597-602.

(22) Kharenko, O. A.; Young, P. R.; Brown, S. D.; Duffy, B.C.; Liu, S.; Guzzo, P. Inhibitors of Bromodomains, 2016, WO/2016/097863.

SYNOPSIS

Table of Contents graphic

Covalent binding of BET inhibitor to BRD4(BD1)

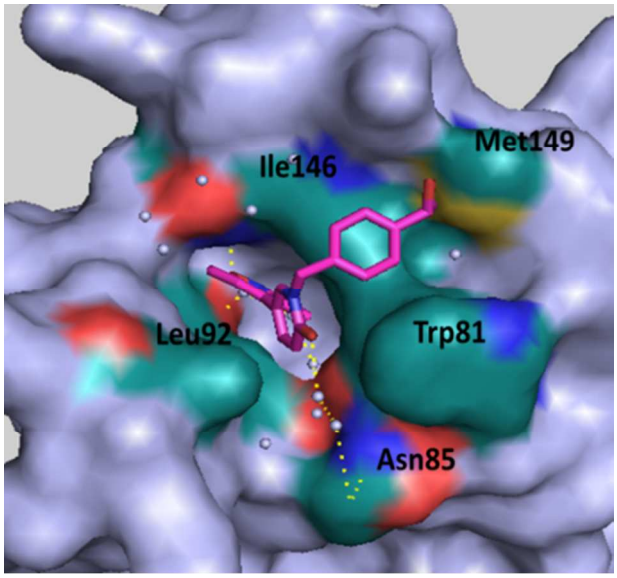

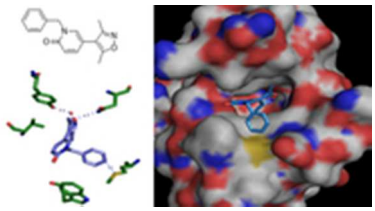

Figure 1. The chemical structure of 1 (ZEN-2759) (top left). Co-crystal structure of BRD4(BD1) and 1, pdb code 6CZV.pdb, showing specific protein-ligand interactions (bottom left) and a surface representation (right).

15x8mm (300 x 300 DPI)

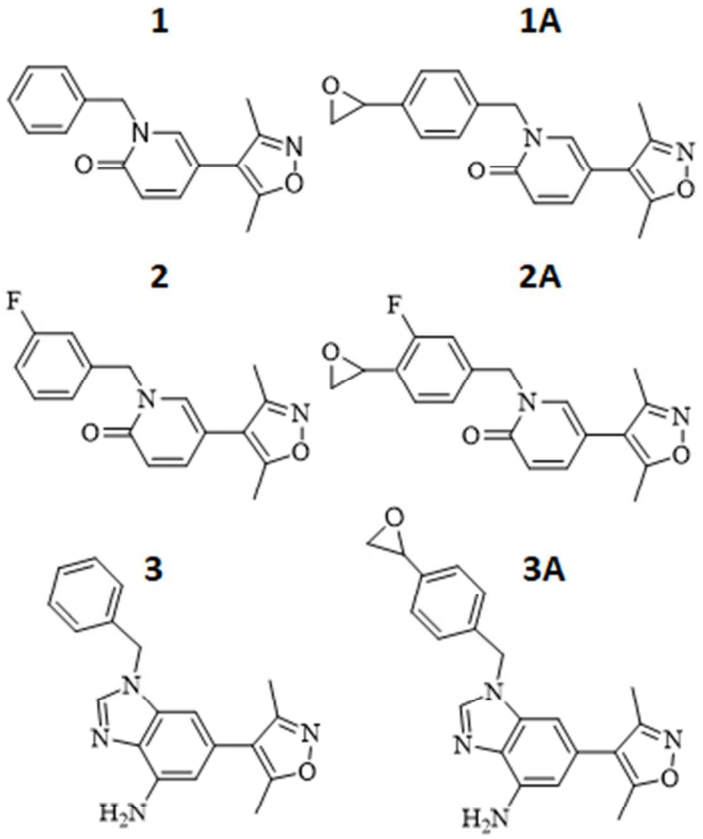

Figure 2. Chemical structures of epoxide containing analogues of BET inhibitors.

42x40mm (300 x 300 DPI)

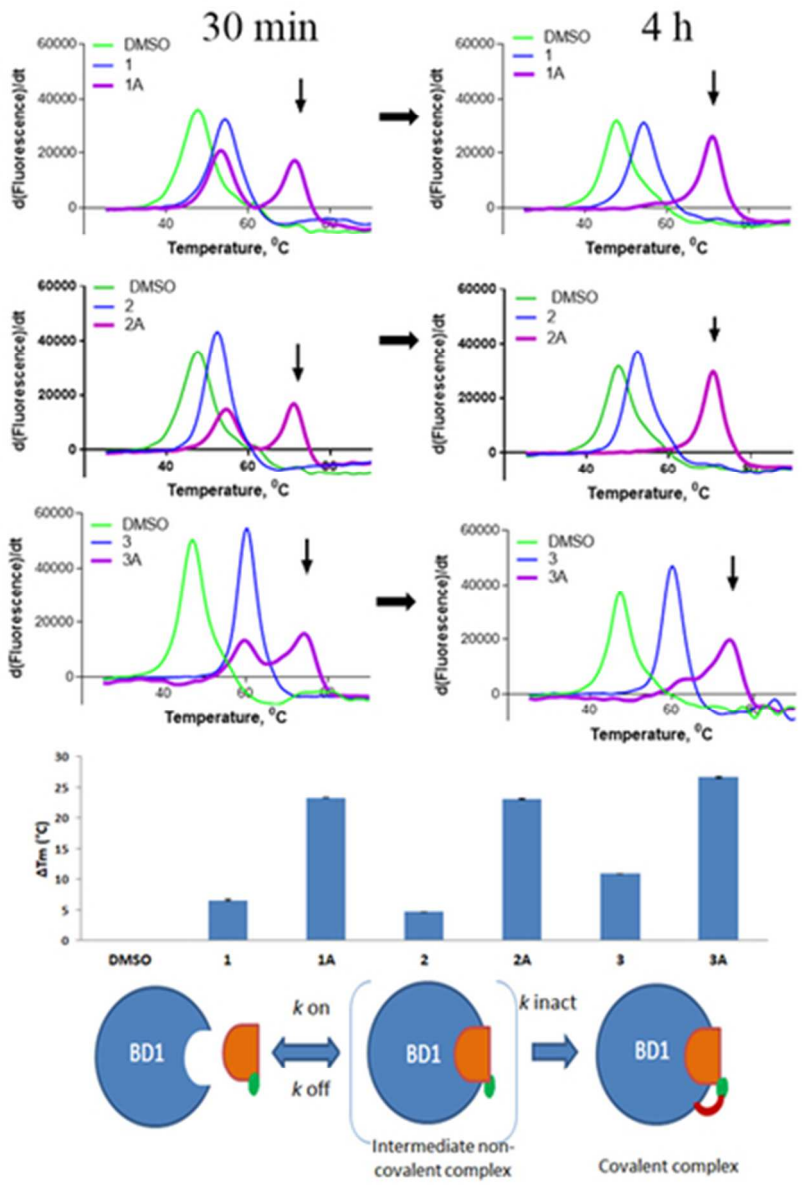

Figure 3. Interaction of BET inhibitors with BRD4(BD1) measured by thermal denaturation assay.

35x50mm (300 x 300 DPI)

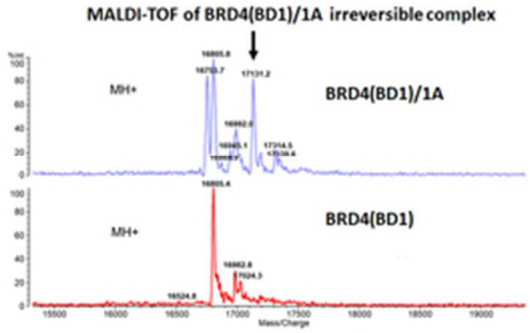

Figure 4. MALDI-TOF spectrometry of 1A/BRD4(BD1) complex vs. apo BRD4(BD1).

23x16mm (300 x 300 DPI)

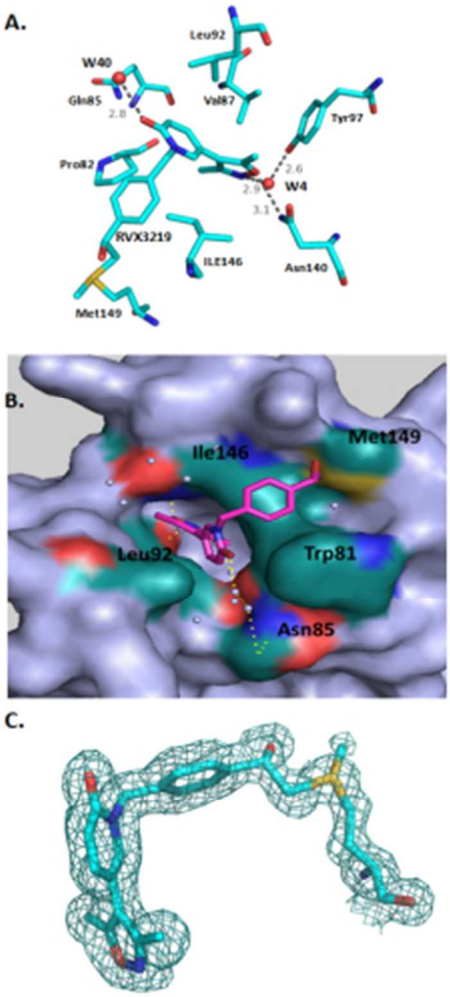

Figure 5. X-RAY co-crystal structure of 1A (ZEN-3219) with BRD4(BD1), pdb code 6CZU.pdb. A. Interacting amino acid residues of BRD4(BD1) with 1A. B. Surface representation of 1A binding mode in BRD4(BD1) binding pocket. C. Electron density map (SigmaA-weighted 2Fo-Fc in teal colour at 1.0 σ contour level) corresponding to compound 1A bound to BRD4(BD1) and a covalent link between the compound and Sγ atom of Met149. D. Ligand Interaction Diagram (LID) demonstrating the covalent interaction of 1A and Met149 of BRD4(BD1). Hydrogen bonds are designated with a dashed line and van der Waals interactions are shown by a half "sun" arrangement.

60x132mm (96 x 96 DPI)

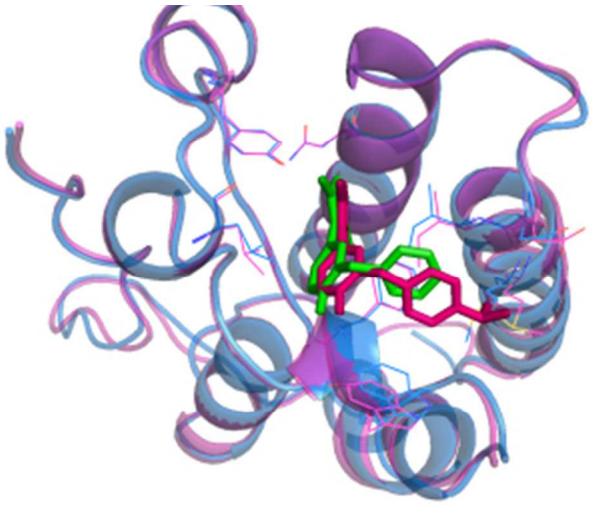

Figure 6. Structural overlay of BRD4(BD1)/1A (pink) and 1 (green).

98x71mm (96 x 96 DPI)

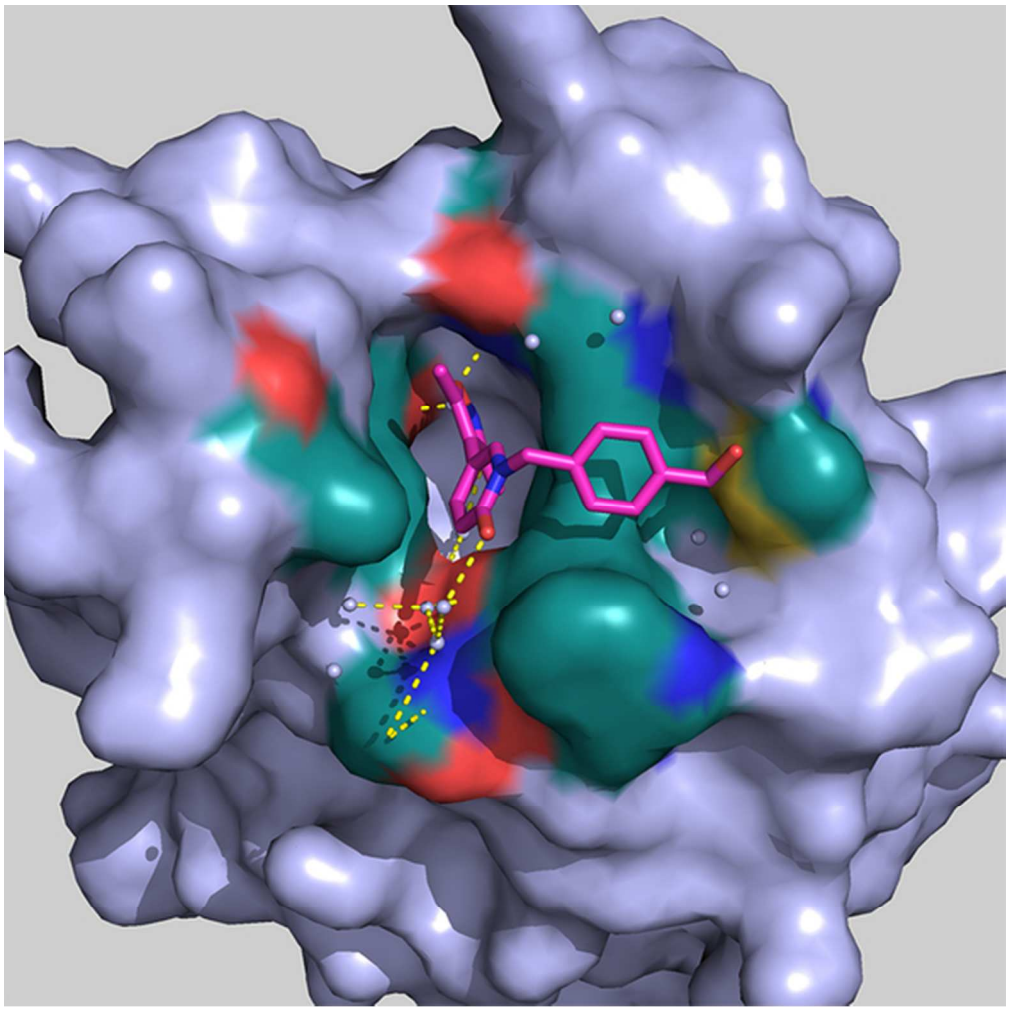

Covalent binding of BET inhibitor to BRD4(BD1)

49x49mm (300 x 300 DPI)